

Synthesis and Induced Micellization of Pd-Containing Polystyrene-*block*-poly-*m*-vinyltriphenylphosphine Diblock Copolymers

Dmitrii M. Chernyshov*

*Nesmeyanov Institute of Organoelement Compounds, Russian Academy of Sciences,
28 Vavilov St., Moscow 117813, Russia*

Lyudmila M. Bronstein

Indiana University, Chemistry Department, Bloomington 47405, Indiana

Hans Börner

Philipps-University Marburg, Hans-Meerwein-Strasse, D-35032 Marburg, Germany

Beate Berton and Markus Antonietti

MPI of Colloids and Interfaces, Am Mühlenberg, D-14424 Potsdam/Golm, Germany

Received July 13, 1999. Revised Manuscript Received October 4, 1999

A novel type of chelating block copolymer, polystyrene-*block*-poly-*m*-vinyltriphenylphosphine (PS-*b*-PPH), was reacted with $(\text{CH}_3\text{CN})_2\text{PdCl}_2$ or $(\text{PPh}_3)_2\text{PdCl}_2$, and the products were examined with FTIR, ^{31}P NMR spectroscopy, and elemental analysis. The complexation of triphenylphosphine groups of these polymers with palladium compounds induces micellization in the system, and no polymer gels were formed. The morphology of the Pd-containing diblock copolymer micelles was studied with transmission electron microscopy (TEM). The size and kind of micellar aggregates depends strongly on the molecular weight of diblock copolymer, its composition, and metal compound type. Block copolymer-stabilized Pd nanoparticles were prepared by reduction of Pd-containing PS-*b*-PPH with $\text{N}_2\text{H}_4\cdot\text{H}_2\text{O}$, $\text{LiB}(\text{C}_2\text{H}_5)_3\text{H}$, and LiAlH_4 and analyzed by TEM, X-ray photoelectron spectroscopy, and wide-angle X-ray scattering techniques. It is found that the morphology of nanoparticles is controlled by the way of reduction and by the nature of the polymeric aggregates.

Introduction

The synthesis of organometallic polymers and the development of polymer composites containing nanoparticles are rapidly developing fields of material science due to their unique catalytic, magnetic, semiconductive, and optical properties.^{1–4} Usually, immobilization of organometallic complexes in polymers becomes possible when metal-interacting functional groups are attached to the polymers. In this context, polymers containing organophosphorus compounds draw a special interest because of their widespread use in coordination chemistry and catalysis.^{4,5} The soft-base character of the phosphorus center combined with its ability to behave as an electron acceptor toward π -back-donation results in both the formation of a vast range of complexes with

transition elements and the stabilization of metal atoms in low formal oxidation states. Immobilization of transition-metal complexes in various phosphorus-containing polymer matrixes is probably one of the most widely applied method for the preparation of highly active and stable polymeric catalysts.^{6,7} Polymer supports traditionally employed for the binding of metal complexes include a variety of macromolecular resins functionalized with different organophosphorus groups.^{8–12} At the same time, only few examples of immobilization of metal complexes in more defined diblock copolymers containing organophosphorus groups are found.^{13–15} In the

* To whom correspondence should be addressed: Dmitrii M. Chernyshov, Nesmeyanov Institute of Organoelement Compounds, 28 Vavilov St., Moscow 117813, Russia. E-mail: dmc@ineos.ac.ru.

(1) Henglein, A. *Chem. Rev.* **1989**, 1861.
(2) Ogawa, S.; Hayashi, Y.; Kobayashi, N.; Tokizaki, T.; Nakamura, A. *Jpn. J. Appl. Phys.* **1994**, 33, L331.
(3) Lewis, L. N. *Chem. Rev.* **1993**, 93, 2693.
(4) *Nanoparticles and Nanostructured Films*; Fendler, J. H., Ed.; Wiley-VCH: Weinheim, New York, 1998; p 468.
(5) McAuliffe, C. A.; Levason, W. *Phosphine, Arsine, and Stibine Complexes of the Transition Elements*; Elsevier: Amsterdam, 1979.

(6) Meek, D. W. *Strem Chem.* **1977**, 5, 3.
(7) Nappier, T. E. Jr.; Meek, D. W.; Kirchner, R. M.; Weinkauff, D. *J. Am. Chem. Soc.* **1975**, 97, 2567.
(8) Pittman, C.; Smith, L.; Hanes, R. *J. Am. Chem. Soc.* **1975**, 97 (7), 1742.
(9) Bruner, H.; Bailar, J. *Inorg. Chem.* **1973**, 12 (7), 1465.
(10) Strukul, G.; Bonivento, M.; Graziani, M. *Inorg. Chim. Acta.* **1975**, 12 (1), 15.
(11) Terasawa, M.; Kaneda, K.; Imanaka, T.; Tranishi, S. *J. Organomet. Chem.* **1978**, 162 (3), 403.
(12) Sunger, A.; Schalling, L.; Tan Gie, K. *Inorg. Chim. Acta.* **1979**, 35 (1), 325.
(13) Antonietti, M.; Förster, S.; Oestreich, S.; Hartmann, J. *Macromolecules* **1996**, 29, 3800.
(14) Antonietti, M.; Förster, S.; Oestreich, S.; Hartmann, J.; Wenz, E. *Nachr. Chem. Lab. Technol.* **1996**, 44, 579.

Table 1. Characteristics of PS-*b*-PPH Block Copolymers^a

polymer	N_{PS}	N_{PPH}	M_n	D
PS- <i>b</i> -PPH1	223	18	2.9×10^4	1.04
PS- <i>b</i> -PPH2	42	6	6.1×10^3	1.11
PS- <i>b</i> -PPH3	740	60	9.3×10^4	1.40

^a N_{PS} is the polymerization degree of the PS block, N_{PPH} is the polymerization degree of the PPH block, M_n is the number-average molecular weight, and D is the ratio M_w/M_n .

present paper, we report on the immobilization of two Pd compounds, $(CH_3CN)_2PdCl_2$ and $(PPh_3)_2PdCl_2$, on polystyrene-*block*-poly-*m*-vinyltriphenylphosphine (PS-*b*-PPH) diblock copolymers containing monomer-bound tertiary phosphine units and on the induced micellization in such systems due to complexation. In addition, we focus on the preparation of Pd nanoparticles by reduction of these micellar precursors and show how the nature of the immobilized palladium complex and the type of reducing agent can influence the structure and chemical composition of final hybrid materials.

Experimental Section

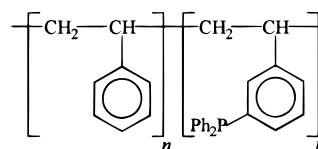
Materials. The PS-*b*-PPH block copolymers were synthesized by anionic polymerization as described elsewhere.^{16,17} The characteristics of block copolymers are summarized in Table 1.

Bis(acetonitrile)palladium(II) chloride $((CH_3CN)_2PdCl_2)$, bis(triphenylphosphine) palladium(II) chloride $((PPh_3)_2PdCl_2)$, hydrazine-hydrate ($N_2H_4 \cdot H_2O$), superhydride ($LiB(C_2H_5)_3H$, SH, 1 M solution in THF), lithium aluminumhydride ($LiAlH_4$, 1 M solution in THF) were obtained from Aldrich and used as received.

THF was purified by refluxing over Na/benzophenone complex. A violet-purple solution indicated moisture- and air-free THF. After that, THF was distilled under argon. Other solvents were obtained commercially and used without further purification.

Preparation of Pd-Containing Polymers and Pd Nanoparticles. Samples of PS-*b*-PPH were dissolved in THF at a concentration of 10 g/L under vigorous stirring for 30 min. The metal compounds were added to the polymer solutions under air and stirred for 24 h at room temperature (molar ratio P/Pd varied from 2/1 to 4/1). After that, the mother solution was filtrated and precipitated with either methanol or petroleum ether. The precipitate was thoroughly washed with methanol and dried for 24 h in a vacuum-desiccator over P_2O_5 . These powderlike, metal salt-containing polymers were easily redissolved in all solvents good for polystyrene (PS). The degree of complexation for organometallic polymers (χ) was calculated from the formula $(m_{Pd}/m_P)(M_P/M_{Pd})N \times 100\%$, where m_{Pd} and m_P are the elemental analysis data on Pd and P, respectively, M_P and M_{Pd} are the atomic weight values, and N is 2 for the $(PR_3)_2Pd$ complex fragment (see Table 2).

Reduction of Pd-containing samples was performed in a two-neck flask equipped with a stopcock, rubber septum, and a Teflon stir bar. Fast-reducing agents such as $LiAlH_4$ and SH were used in a 2.6-fold excess; $N_2H_4 \cdot H_2O$ was used in a 5-fold excess. In all cases, reduction was carried out under argon after a standard degassing procedure.¹⁸ The use of degassed samples during reduction provides the stability of Pd nanoparticle solutions under air. Isolation of the block copolymer-

Scheme 1

stabilized Pd nanoparticles was achieved by precipitation with petroleum ether, filtration, and drying for 24 h in a vacuum desiccator over P_2O_5 .

Measurements. FTIR spectra were recorded with a Nicolet FTIR spectrometer on KBr pellets in the spectral region of 500–100 cm^{-1} with a resolution of 2 cm^{-1} . ^{31}P NMR spectra were recorded with a Bruker WP-200 SY at a frequency of 200 MHz. Positive chemical shifts were downfield from 85% H_3PO_4 .

Samples for transmission electron microscopy (TEM) were prepared by evaporation of 10^{-4} mol/L THF solutions under air. Electron micrographs of the samples were obtained with a Zeiss 912 Omega electron microscope. Wide-angle X-ray scattering (WAXS) measurements were performed with Nonius PDS120 powder diffractometer in transmission geometry.

X-ray photoelectron spectroscopy (XPS) was carried out with a two-chamber XSAM-800 spectrometer (Kratos, U.K.). For photoelectron excitation, the characteristic Mg $K\alpha$ radiation was used; the power ($h\nu = 1253.6$ eV) of the X-ray gun did not exceed 75W (15 kV, 5 mA). The spectra were recorded at a pressure of 10^{-9} Torr. Samples for XPS analysis were prepared by precipitation of Pd-containing colloidal solutions with degassed petroleum ether, filtration under Ar, and drying in a vacuum desiccator at 0.5 mbar overnight.

Results and Discussion

For metal binding, three highly asymmetric PS-*b*-PPH diblock copolymers (Scheme 1) were synthesized (Table 1). All of them consist of a rather short block containing diphenylphosphine groups, which are supposed to interact with metal compounds, and a comparatively long PS block, which should be indifferent to complexation and is designed to solvate the complexation and reaction site in solution. For block copolymers 1 and 3 (Table 1), the PS block is longer than PPH by a factor of 12, but the molecular weights of these two block copolymers differ by a factor of 3. The PS-*b*-PPH2 block copolymer has a molecular weight of only 6100 and a block ratio of 7. The use of these block copolymers is intended to clarify the influence of different block length and composition on complexation with Pd compounds.

Commonly, the synthesis of metal-containing polymers is carried out by ligand exchange reaction of low-molecular-weight ligands (e.g., nitrile, olefin, phosphine and so on) in the corresponding transition-metal complex with the appropriate organophosphorus polymer groups.^{19,20} Similarly, for complexation with PS-*b*-PPH diblock copolymers, bis(triphenylphosphine) palladium chloride $((PPh_3)_2PdCl_2)$, and bis(acetonitrile)palladium chloride $((CH_3CN)_2PdCl_2)$ were chosen. For $(CH_3CN)_2PdCl_2$, the driving force for a ligand exchange reaction with polymer phosphine groups is a formation of more stable complex; that is, it is thermodynamically favorable along with entropy gain related to increase of the molecule amount. For $(PPh_3)_2PdCl_2$, ligand exchange is presumed to be driven by solely entropy: immobilization of complexes in polymers is favorable compared to complexation with small molecules.

(15) Kabachii, Y.; Bronstein, L.; Bol'shakova, M.; Valetsky, P. *Polymer* **1999**, in press.

(16) Antonietti, M.; Heinz, S.; Rosenauer, C.; Schmidt, M. *Macromolecules* **1994**, *27*, 3276.

(17) Förster, S.; Ziesenis, M.; Wenz, E.; Antonietti, M. *J. Chem Phys.* **1996**, *104*, 9956.

(18) Antonietti, M.; Wenz, E.; Bronstein, L.; Seregina, M. *Adv. Mater.* **1995**, *7* (12), 1000.

(19) Teresawa, M.; Kaneda, K.; Imanaka, T.; Teranishi, S. *J. Catalysis* **1978**, *51*, 406.

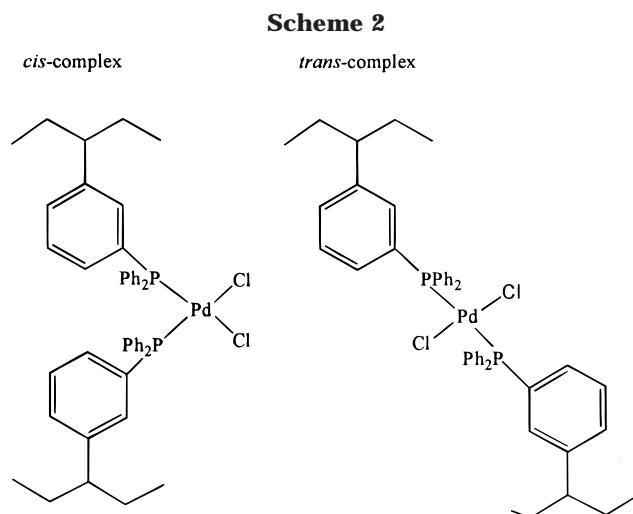
(20) Bruner, H.; Bailar, J. C. *Inorg. Chem.* **1973**, *12*, 1465.

Table 2. Composition and Characteristics of Pd-containing PS-*b*-PPH

polymer	metal compound used	elemental analysis data (%)					χ (%)	ν (Pd-Cl) (cm ⁻¹)	chemical shift (ppm vs. H ₃ PO ₄)
		Pd	Cl	P	C	H			
PS- <i>b</i> -PPH1-Pd1	(CH ₃ CN) ₂ PdCl ₂	4.80	3.72	3.66	80.4	6.62	76.6	360, 364	+24.0, +33.3
PS- <i>b</i> -PPH1-Pd2	(PPh ₃) ₂ PdCl ₂	5.18	4.00	3.86	79.0	6.49	88.1	358	+25.6
PS- <i>b</i> -PPH2-Pd1	(CH ₃ CN) ₂ PdCl ₂	4.90	3.77	3.71	79.8	6.54	80.2	358, 364	+23.9, +33.2
PS- <i>b</i> -PPH2-Pd2	(PPh ₃) ₂ PdCl ₂	5.16	3.98	3.82	80.1	6.65	85.8	357	+25.6
PS- <i>b</i> -PPH3-Pd1	(CH ₃ CN) ₂ PdCl ₂	4.87	3.74	3.61	80.5	6.57	79.2	358, 362	+23.7, +33.1
PS- <i>b</i> -PPH3-Pd2	(PPh ₃) ₂ PdCl ₂	5.21	4.02	3.80	79.4	6.49	79.6	358	+25.7

^a Molar ratio of P/Pd (mol) in all of the polymer samples is 2/1; χ is the degree of complexation.

Pd-Containing Polymers Derived from Bis(acetonitrile)palladium Chloride. The interaction of bis(benzonitrile)palladium chloride with low-molecular-weight phosphines is known to result in the formation of chlorine-bridged dinuclear Pd complexes.²¹ At the same time, by published data, the immobilization of Pd complexes containing labile ligands (acetonitrile, benzonitrile) in polymers with phosphine groups results in the formation of mononuclear mono- and disubstituted products.^{19,20} To examine the structure of PS-*b*-PPH containing Pd complexes, FTIR spectra were recorded in the range of 500–100 cm⁻¹ (far-IR), where bands characteristic of metal–chlorine bonds can be observed. It was intended to clarify the question of whether terminal or chlorine-bridged ligands are present in the complex. The far-IR spectrum of the sample derived from PS-*b*-PPH1 and (CH₃CN)₂PdCl₂ (PS-*b*-PPH1-Pd1, molar ratio P/Pd = 2/1) displays two bands at 360 and 364 cm⁻¹, which can be assigned to the terminal chlorine ligands.^{22,23} An increase of the P/Pd molar ratio from 2/1 to 4/1 does not result in the appearance of any new bands in the far-IR region. The ³¹P NMR spectrum of the PS-*b*-PPH1-Pd1 sample exhibits complete vanishing of a signal characteristic of polymeric *m*-vinyltriphenylphosphine units with a -5.5 ppm chemical shift and the appearance of new broad signals with chemical shifts of +24.0 and +33.3 ppm (relative intensity of signals 1/4, respectively). According to Grim and Keiter,²⁴ ³¹P chemical shifts of low-molecular-weight *cis*-Pd(II) complexes are always upfield compared to the *trans* isomers. We suggest that the signal at +33.3 ppm corresponds to the *cis* isomer, and the signal at +24.0 ppm can be assigned to the *trans* isomer structure. The presence of both *cis* and *trans* forms can be explained by the spontaneous isomerization, which is usually observed for dialkylphenyl- and alkyl-diphenylphosphine Pd complexes even in the absence of an excess of a free phosphine ligand.²⁴ All of the Pd-containing PS-*b*-PPH1 species are well-soluble in THF, which is typical for appropriately designed block copolymers (the solubility is maintained even for intermolecular complexation due to micellization of block copolymers).^{25,26} By elemental analysis, PS-*b*-PPH1-Pd1 contains 4.80 wt % Pd and



3.72 wt % Cl, which exactly correlates with that of the PdCl₂ fragment. Thus, relying on FTIR, ³¹P NMR, and elemental analysis, we can suggest the structure in Scheme 2 for the corresponding PS-*b*-PPH1-Pd1 complexes.

Pd-Containing Polymers Derived from (PPh₃)₂-PdCl₂. Pd-containing diblock copolymers derived from PS-*b*-PPH1 and (PPh₃)₂PdCl₂ (PS-*b*-PPH1-Pd2) have been prepared using a molar ratio of P/(PPh₃)₂PdCl₂ = 2/1. The FTIR spectrum of PS-*b*-PPH1-Pd2 in the far-IR region exhibits one strong band at 358 cm⁻¹, which can be ascribed to the terminal Cl ligands.²² In the ³¹P NMR spectrum of PS-*b*-PPH1-Pd2, one signal with the chemical shift of +25.6 ppm was registered, but a signal characteristic of free polymer-bound triphenylphosphine groups was not observed. Thus, the intense and broad signal at +25.6 ppm can be assigned to the block copolymer organophosphorus units taking part in complexation with (PPh₃)₂PdCl₂. The value of the ³¹P chemical shift allows the suggestion that, unlike (CH₃CN)₂PdCl₂, immobilization of (PPh₃)₂PdCl₂ results in the formation of solely *trans*-substituted macromolecular complexes (Scheme 2). The elemental analysis data of PS-*b*-PPH1-Pd2 (5.18 wt % of Pd and 4.0 wt % of Cl) accurately correspond to the presence of the PdCl₂ fragment.

The structural characteristics and composition of the various PS-*b*-PPH diblock copolymers with immobilized Pd complexes are summarized in Table 2.

Morphological Study of the Pd-Containing PS-*b*-PPH Diblock Copolymers. Because interaction of (PPh₃)₂PdCl₂ or (CH₃CN)₂PdCl₂ with PS-*b*-PPH diblock copolymers results in soluble organometallic polymers, it was surmised that intermolecular complexation and cross-linking lead to the formation of finite polymer

(21) Chatt, J.; Venanzi, L. *J. Chem. Soc.* **1957**, 2351.

(22) Nakomoto, K. In *Infrared and Raman Spectra of Inorganic and Coordination Compounds*; John Wiley and Sons: New York, 1986; p 360.

(23) Goodfellow, R.; Goggin, P.; Venanzi, J. *J. Chem. Soc. A* **1967**, 1897.

(24) Grim, S. O.; Keiter, R. L. *Inorg. Chim. Acta.* **1970**, 4 (1), 56.

(25) Bronstein, L.; Sidorov, S.; Gourkova, A.; Valetsky, P.; Hartmann, J.; Bruelmann, M.; Cölfen, H.; Antonietti, M. *Inorg. Chim. Acta.* **1998**, 280, 348.

(26) Bronstein, L.; Seregina, M.; Platonova, O.; Kabachii, Y.; Chernyshov, D.; Ezernitskaya, M.; Dubrovina, L.; Bragina, T.; Valetsky, P. *Macromol. Chem. Phys.* **1998**, 199, 1357.

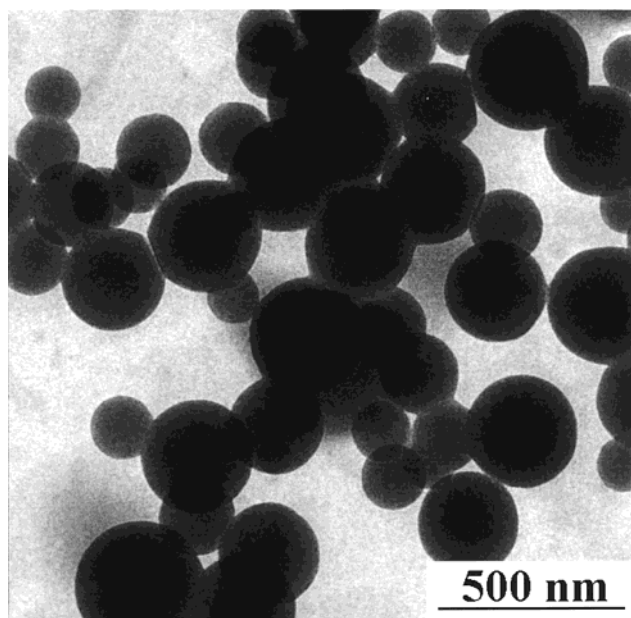


Figure 1. TEM micrograph of the Pd-containing polymer derived from PS-*b*-PPH1 and $(\text{CH}_3\text{CN})_2\text{PdCl}_2$. Molar ratio P/Pd = 2/1.

superstructures, such as micelles, where the cross-linked PPH blocks form the micelle core, whereas the soluble PS blocks form the micelle corona. A similar phenomenon was observed in previous work for the complexation of Pd, Pt, and Rh compounds with polystyrene-*block*-polybutadiene diblock copolymer.²⁴ To characterize the morphology of Pd-containing PS-*b*-PPH diblock copolymers, TEM was employed.

In the TEM micrograph of PS-*b*-PPH1-Pd1 (Figure 1) derived from $(\text{CH}_3\text{CN})_2\text{PdCl}_2$ (molar ratio P/Pd = 2/1) one can see well-defined spherical aggregates having different morphology. The diameter of aggregates is rather large and varies between 70 and 400 nm. A careful look at the micrograph allows one to distinguish between compact spheres with the typical increase of the electron density toward the center and the objects that look evenly gray and can be ascribed to disklike micelles.

Disklike micelles were already found for different rod-coil copolymers.²⁷ Similar micellar aggregates were also theoretically predicted for polymers containing strongly interacting groups in short blocks,²⁸ which are expected to follow the laws of the so-called superstrong segregation regime in polymers. In our case, the formation of the disklike aggregates in the reaction solution can be caused by the fast formation of $\text{PdCl}_2(\text{PPh}_3)_2$ complexes between the short PPH blocks belonging to different polymeric chains. It is speculated that the fast complexation provided by the easy substitution of acetonitrile ligands with phosphine groups results in a phenomenon that we call "zippering" of the interacting blocks with each other, which consecutively super-assemble to a disklike micelle core (see Figure 2a).

A disklike architecture also goes well with the size of the polymer chains (60.5 nm contour length) that is definitely too small to explain the radius of the observed

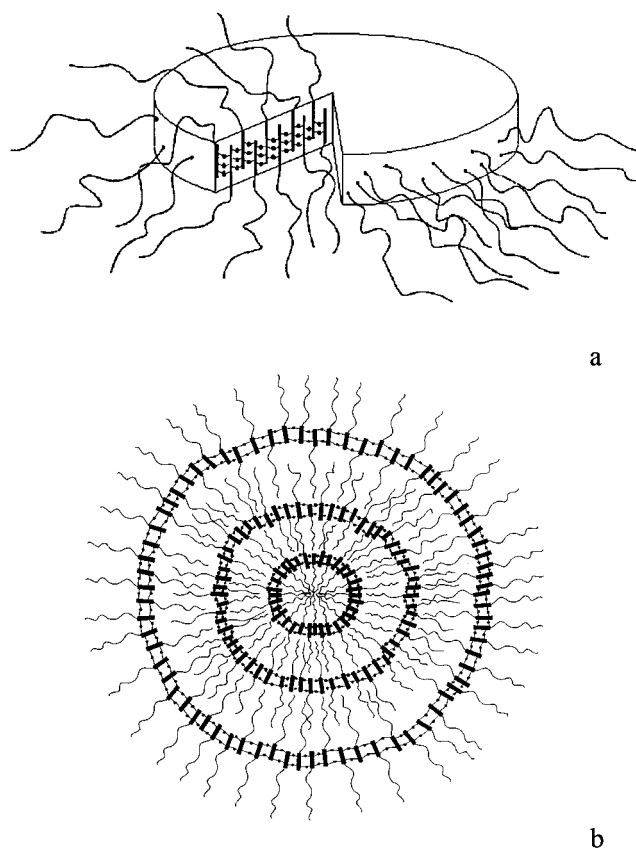


Figure 2. Schematic images of the disklike (a) and multi-lamellar vesicles (b).

aggregates when a simple spherical micelle is assumed. For discotic micelles, it is the thickness that is related to the molecular dimensions, and there are no limits for the lateral extensions. Within this discussion, we also have to exclude a simple micellar architecture for the compact spherical objects, and both multilamellar vesicles (Figure 2b) or multicore micellar aggregates can explain the found electron density profiles. Because both structures coexist, the multilamellar vesicle is the more probable case (both disks and multilamellar vesicles belong to the class of lamellar architectures).

A strong hint that this attribution is correct is obtained by variation of the density of metal complexes and therefore the geometrical constraints. Morphological changes are found to occur with decreases in the $(\text{CH}_3\text{CN})_2\text{PdCl}_2$ loading (molar ratio P/Pd = 4/1). Along with the already known multilamellar vesicles and disks, both unilamellar vesicles and "perforated hulls" appear in the TEM image (Figure 3).

These two architectures also belong to the class of lamellar morphologies and are always found in close proximity to physical parameters of the two others. A decrease of the complex density obviously results in looser packing of the polymer chains and in the formation of objects as unilamellar vesicles.

It should be mentioned that similar block copolymer assembly architectures were also observed for "crew-cut" aggregates derived from polystyrene-*block*-poly(acrylic acid) (PS-*b*-PAA).²⁹ According to Zhang et al.,²⁹

(27) Raphael, E.; de Gennes, P.-G. *Physica A* **1991**, *177*, 294.

(28) Semenov, A. N.; Nyrkova, I. A.; Khokhlov, A. R. *Macromolecules* **1995**, *28*, 7491.

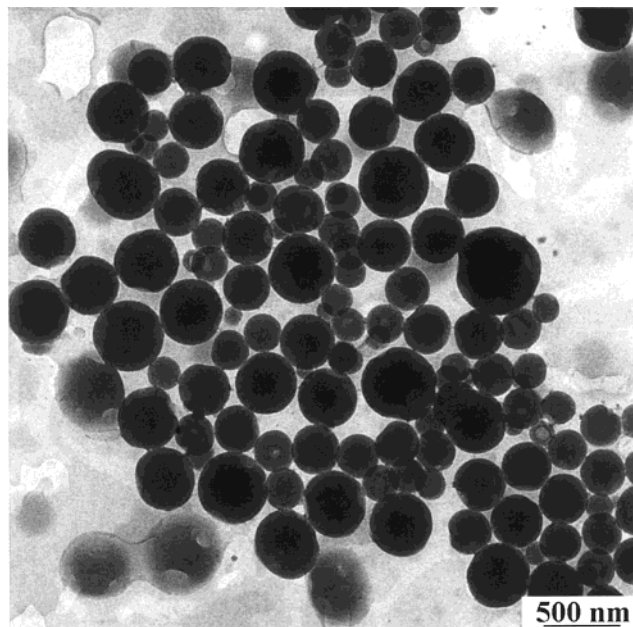


Figure 3. TEM micrograph of the Pd-containing polymer derived from PS-*b*-PPH1 and $(\text{CH}_3\text{CN})_2\text{PdCl}_2$. Molar ratio P/Pd = 4/1.

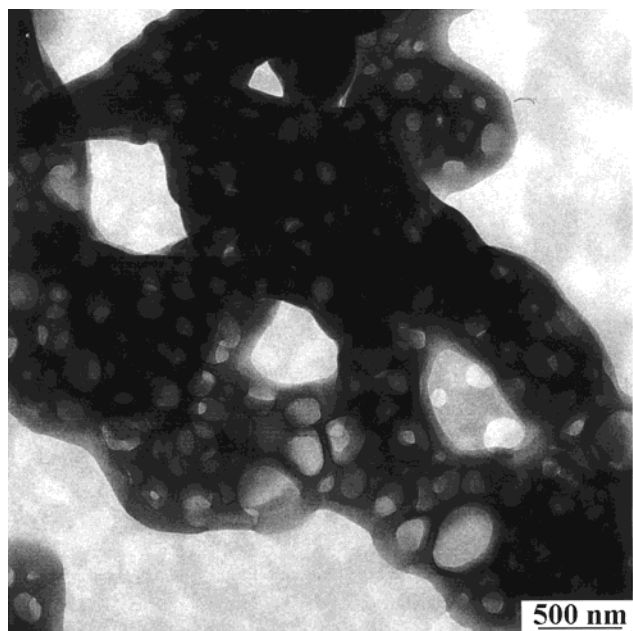


Figure 4. TEM micrograph of the Pd-containing polymer derived from PS-*b*-PPH1 and $(\text{PPh}_3)_2\text{PdCl}_2$. Molar ratio P/Pd = 2/1.

the morphological changes were induced by small changes in the ionic strength of the aqueous solvent. It must be underlined that in the case of the crew-cuts the block length ratio is inverted: the solvating block is much shorter compared with the architecture forming block. Commonly, it is assumed that block copolymers as used in our work with a small insoluble block have to form small spherical micelles.¹⁷ Thus, cross-linking between short blocks and the resulting geometric and energetic constraints lead to a new assembly scenario, as it was previously found only for block copolymers with one rodlike block.

Figure 4 underlines the sensitivity of the resulting assembly process toward minor changes of the geometry of the complexes and polymer–polymer interactions: it depicts the superstructures of the block copolymer complexes derived from PS-*b*-PPH1 and $(\text{PPh}_3)_2\text{PdCl}_2$ and prepared at molar ratio P/Pd = 2/1.

In this case, one can see a stable, foamlike morphology that consists of a vesicular elements forming a network. This type of morphology was also found for a crew-cut polymer (PS(410)-*b*-PAA(25) in the presence of HCl)²⁹ and was called “large compound vesicles” (LCVs). In our case, the irregularly cross-linked PPH blocks form soft walls of the vesicular aggregates, whereas their outer surface and “holes” are lyophilic due to the presence of the PS chains.

Thus, it became quite clear that morphology of Pd-containing polymers is strongly affected by the nature of palladium compound. It was already said that one major difference is the (local) structure of the formed complexes: for $(\text{CH}_3\text{CN})_2\text{PdCl}_2$, cis complexes prevail (the ratio between cis and trans complexes is 4/1), whereas for $(\text{PPh}_3)_2\text{PdCl}_2$, a predominant trans state is found by spectroscopy. From Scheme 2, it becomes obvious that this difference results in a different packing structure of the PPH chains during complexation, which again is reflected in the superstructure. Another reason for the differences can be a kinetic one: it can be assumed that the slower exchange of low-molecular-weight phosphine ligands in $(\text{PPh}_3)_2\text{PdCl}_2$ for similar phosphine groups of polymer compared to the ligand exchange in reaction with bis(acetonitrile)palladium chloride results in a more optimized intermolecular packing of the block copolymer structures (on the level of the polymers), leading to a more equilibrated structure and the absence of polymorphism. At this point of the discussion, it is not possible to evaluate the relative importance of both contributions.

On the other hand, we can exclude the influence of a monosubstituted $[-\text{PPh}_2(\text{PPh}_3)\text{PdCl}_2]$ species (for $(\text{PPh}_3)_2\text{PdCl}_2$), which, in principle, can take place, but was not observed experimentally, as can be seen from Table 2. Indeed, the existence of monosubstituted species was supposed to strongly increase the P and C content in the end polymer, decreasing the Pd and Cl content, because for each complex an additional diphenyl phosphine ligand would appear. However, comparison of elemental analysis data for polymers obtained from $(\text{PPh}_3)_2\text{PdCl}_2$ and $(\text{CH}_3\text{CN})_2\text{PdCl}_2$ does not display such a tendency.

Practically the same results were obtained for Pd-containing block copolymers derived from PS-*b*-PPH2, although this block copolymer is by a factor of 5 lower in molecular weight and slightly less asymmetric. The same structure patterns were found, where all the structures belong to the family of lamellar morphologies. Moreover, the typical overall diameters of the smallest spheres are 3 times smaller, whereas large aggregates (up to about 400 nm) are of the same size. This is in good agreement with the size of the constituting units, which should influence only the size of small aggregates, whereas the size of large multilamellar structures should be determined in terms of overall aggregate stability. This is important to note, because it underlines that the overall morphology does not respond to block

(29) Zhang, L.; Yu, K.; Eisenberg, A. *Science* **1996**, *272*, 1777.

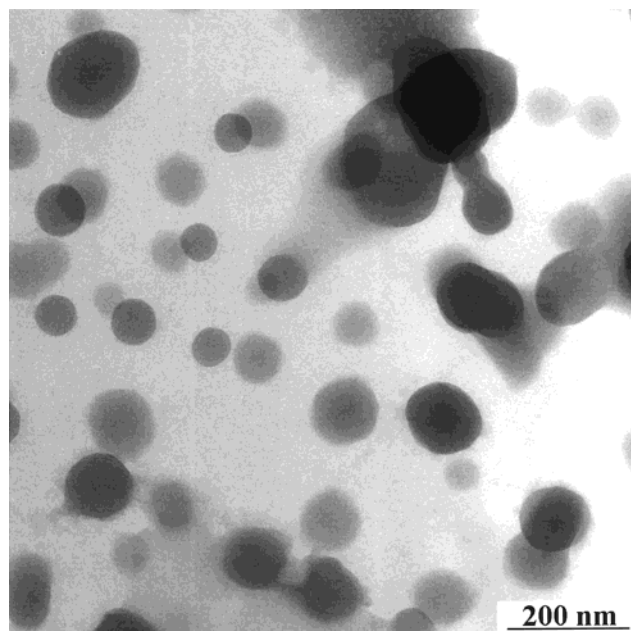


Figure 5. TEM micrograph of the Pd-containing polymer derived from PS-*b*-PPH3 and $(\text{PPh}_3)_2\text{PdCl}_2$. Molar ratio P/Pd = 2/1.

length and block length ratio, as predicted by the classical assembly theory.^{17,30} On the contrary, the architecture does respond to the local geometry and packing of the complexes. The TEM images for this block copolymer are not presented here due to the resemblance of the phenomena.

The block copolymer with the highest molecular weight (PS-*b*-PPH3) shows a related but slightly different behavior. The complexation with $(\text{CH}_3\text{CN})_2\text{PdCl}_2$ proceeds similar to that of PS-*b*-PPH1, but the interaction with phosphine complex results in nearly spherical aggregates. The resulting TEM image of the structures derived from $(\text{PPh}_3)_2\text{PdCl}_2$ and PS-*b*-PPH3 and prepared at molar ratio P/Pd = 2/1 is depicted in Figure 5.

The diameter of the spherical aggregates (the smallest ones) is in the range of 50–70 nm, in coexistence with some larger structures of irregular shape. The radius of the objects does not exceed the order of an extended polymer chain for PS-*b*-PPH3 and therefore is too small for a vesicle, but it is exactly the right size for a spherical micelle. From the present data, it cannot be judged if the micellar core is disklike (as predicted by the super-strong segregation theory)²⁸ or spherical. This is obviously the case that the mutual osmotic repulsion of the longer solvating chains has grown strong enough to disintegrate the larger assembly structures, found for the shorter polymers, into smaller objects.

Metal Colloid Formation in the PS-*b*-PPH Diblock Copolymers. It is known from the literature that the rate of reduction strongly influences the morphology and size of metal nanoparticles formed in the block copolymer aggregates.^{31,32} Fast-working reducing agents were found to induce the formation of

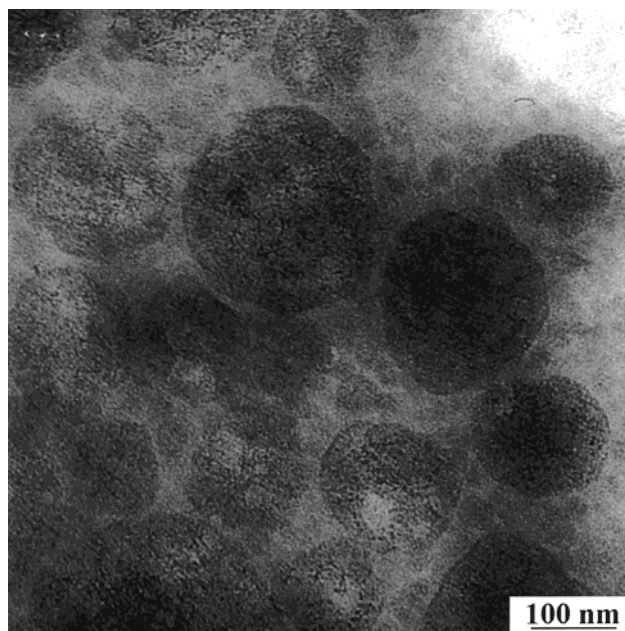


Figure 6. TEM micrograph of Pd nanoparticles prepared by the SH reduction of the Pd-containing polymer derived from PS-*b*-PPH1 and $(\text{CH}_3\text{CN})_2\text{PdCl}_2$ (molar ratio P: Pd = 2/1).

many small particles in micelle, whereas slow-acting reducing agents generated the formation of one or several larger particles per the micelle core. In the present case, addition of fast-working reducing agents such as $\text{LiB}(\text{C}_2\text{H}_5)_3\text{H}$ (SH) and NaBH_4 to the solution of Pd-containing polymer derived from $(\text{CH}_3\text{CN})_2\text{PdCl}_2$ (P/Pd = 2/1) results in the immediate change of color from yellow to black that is characteristic for the formation of Pd colloids. All three types of block copolymers are excellent stabilizers for the formed Pd nanoparticles: the colloidal solutions remained stable without visible changes for long time even after exposure to oxygen. The TEM micrographs of the sample prepared by reduction of the PS-*b*-PPH1–Pd1 complex with SH indicate the presence of very small (1–2 nm) Pd nanoparticles, which are isolated from each other by the embedding in the bodies of the block copolymer aggregates. Block copolymers are weakly contrasted from the background pattern as shadows (Figure 6). Such a morphology of the hybrid together with the electronic properties of the phosphine ligands makes those hybrids very interesting for catalytic applications. It should be noticed that the size of the palladium particle-containing aggregates corresponds to those shown in Figure 1 for the nonreduced sample.

Addition of hydrazine-hydrate to the Pd-containing block copolymer samples results in a much slower change of the color of reaction solution from yellow to black and formation of rather large metal nanoparticles of irregular shape with mean diameters of 7 ± 2 nm. The cause of this phenomenon is a large difference in the kinetics of metal particle nucleation and particle growth for both reduction agents. To accomplish a structural characterization of Pd nanoparticles, WAXS was employed. The X-ray diffractogram is perfectly described by a superposition of an amorphous halo coming from a polymeric matrix and the cubic crystal structure of Pd in the colloids. A quantitative fit of the line width results in a crystalline size of 6.5 ± 0.2 nm,

(30) Förster, S.; Antonietti, M. *Adv. Mater.* **1998**, *3*, 195.

(31) Bronstein, L.; Antonietti, M.; Valetsky, P. In *Nanoparticles and Nanostructured Films*; Wiley-VCH: Weinheim, 1998; p 145.

(32) Seregina, M.; Bronstein, L.; Platonova, O.; Chernyshov, D.; Valetsky, P.; Hartmann, J.; Wenz E.; Antonietti, M. *Chem. Mater.* **1997**, *9*, 923.

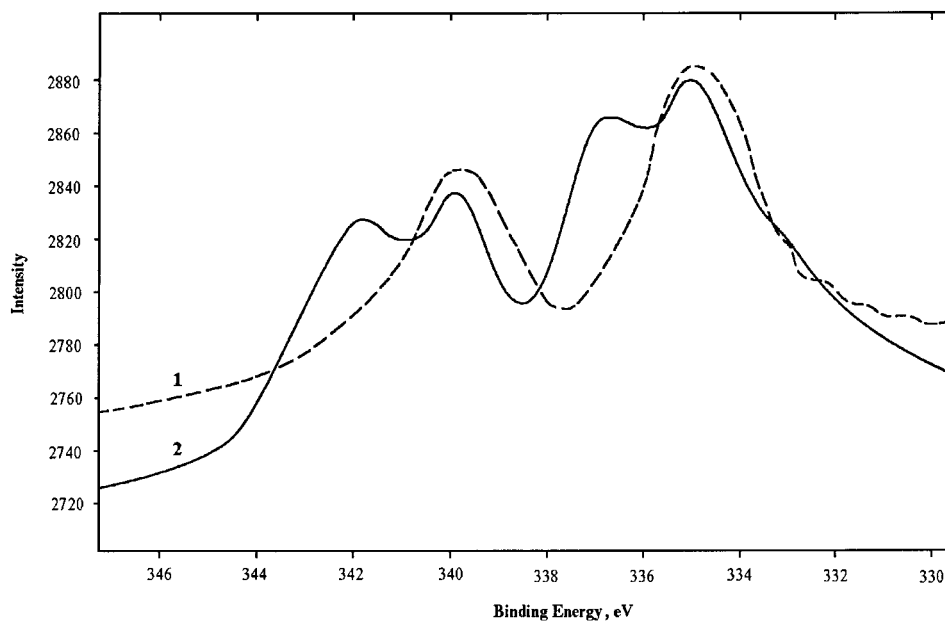


Figure 7. Mg K α XPS spectra of Pd nanoparticles prepared via the SH reduction of the Pd-containing polymer derived from PS-*b*-PPH1 and (CH₃CN)₂PdCl₂ (curve 1) or (PPh₃)₂PdCl₂ (curve 2). Molar ratio P/Pd = 2/1.

which is in good agreement with electron microscopy data. These data are rather typical for Pd-containing polymer films and block copolymers and reflect the reduction conditions rather than a peculiar phosphine polymer effect.^{31,32}

Quite unusual results were obtained for SH and LiAlH₄ reduction of Pd-containing polymer species derived from (PPh₃)₂PdCl₂. In this case, the addition of reducing agent to the Pd-containing diblock copolymer solutions results in an unexpected and very slow change of color from yellow to dark orange and finally to deep red, which takes nearly 30 min. The corresponding electron micrographs showed no particles at all, as there were no pronounced peaks found in the WAXS measurements. To investigate this phenomenon more thoroughly, the resulting reduced Pd-containing species were examined with XPS.

Figure 7 compares the Mg K α spectra of the Pd species obtained via SH reduction of Pd-containing PS-*b*-PPH1 polymer samples derived from (CH₃CN)₂PdCl₂ (curve 1) and (PPh₃)₂PdCl₂ (curve 2). The XPS spectrum of PS-*b*-PPH1-Pd1 (curve 1) exhibits two peaks with binding energies of E3d_{5/2} = 335.2 and E3d_{3/2} = 340.4 eV, characteristic of zerovalent palladium.³³ The XPS spectrum of PS-*b*-PPH1-Pd2 indicates the presence of two doublets with nearly equal intensity. Judging by the position, the bands at E3d_{5/2} = 335.3 and E3d_{3/2} = 340.2 eV can again be attributed to the Pd(0) species, whereas the two other bands at E3d_{5/2} = 337.3 and E3d_{3/2} = 343.3 eV match to Pd(II). Because reduction of Pd-containing polymers was always carried out with excessive amounts of SH, the presence of Pd(II) species cannot be explained by incomplete reduction.

It must be assumed that PS-*b*-PPH1-Pd2 represents the formation of rather stable immobilized Pd-hydride complexes with mixed valency.³⁴ It was possible to

establish the formation of Pd-hydride species by its characteristic FTIR resonance band at 2065 cm⁻¹ found in a freshly reduced PS-*b*-PPH1-Pd2 solution.³⁵ In addition, reaction of the initial (PPh₃)₂PdCl₂ complex with SH in the absence of diblock copolymer results in the same characteristic color change (from yellow to red). The low-molecular-weight reaction mixture was stable under Ar; however, formation of Pd black was observed within several minutes after exposure to air. In contrast, PS-*b*-PPH1-Pd2 solution being exposed to the air showed only slight darkening of the red color without precipitation. Thus, it might be assumed that the presence of stabilizing polymer matrix provides stability of both the hydride metal complex and the Pd clusters, the product of the hydride complex decomposition.

It should be noted that the only chemical difference between complexes derived from (CH₃CN)₂PdCl₂ and (PPh₃)₂PdCl₂ is the occurrence of cis and trans structures. According to the published data, substitution of Cl atoms for H atoms via treatment of Pd compounds with metal hydrides is favorable when the ligands are located in trans position toward the electron-withdrawing groups.³⁶ It must be supposed that the same reaction selectivity is observed for the Pd-containing diblock copolymers. Thus, structure of Pd complexes immobilized in a polymeric matrix can also strongly influence both its reduction pathway and the nature of the species formed.

Conclusions

Novel Pd-containing polymers were synthesized by interaction of polystyrene-*block*-poly-*m*-vinyltriphenylphosphine block copolymers with (CH₃CN)₂PdCl₂ or

(33) Wagner, C.; Riggs, W.; Davis, L.; Mullenberg, G. *Handbook of X-ray Photoelectron Spectroscopy*; Perkin-Elmer Corporation: Minnesota, 1978; p 110.

(34) Seligson, A.; Trogler, W. *Organometallics* **1993**, *12*, 738.

(35) Kudo, K.; Hidai, M.; Murayama, T.; Uchida, Y. *J. Chem. Soc. Chem. Commun.* **1970**, 1701.

(36) *Comprehensive Organometallic Chemistry*; Pergamon Press: Oxford, New York, 1982; Vol. 6, p 1043.

(PPh₃)₂PdCl₂ and examined with ³¹P NMR, FTIR, elemental analysis, and TEM. For both compounds, only mononuclear Pd phosphine complexes were found in polymers; however, their structure depends on the Pd compound used. For (CH₃CN)₂PdCl₂, *cis*-bis(triphenylphosphine) dichloride Pd complexes prevail in the mixture, whereas for (PPh₃)₂PdCl₂, solely *trans* complexes were indicated. The formation of intermolecular complexes in Pd-containing polymers was established to result in an organized induced aggregation of block copolymers forming finite species, avoiding the gelation in the system due to complex polymer network formation.

The aggregate structure induced by the Pd-complexes was found to depend strongly on the composition of initial diblock copolymer and nature of the Pd compound used. A complexation of (CH₃CN)₂PdCl₂ with PS-*b*-PPH of medium molecular weight ($M_w = 2.9 \times 10^4$) was found to result in the formation of spherical aggregates, presumably multilamellar vesicles, disklike micelles, and unilamellar vesicles. In contrast, the interaction of

bis(triphenyl phosphine) Pd complex with the same block copolymer induces the formation of large multivesicular structures of high uniformity.

The PS-*b*-PPH block copolymer micellar aggregates were studied as a stabilizing media for Pd nanoparticle preparation. Analysis of experimental data suggests that size and architecture of Pd colloids strongly depend on the nature of reducing agent and molecular structure of the Pd complex formed in block copolymer. For SH reduction of the species containing solely *trans*-bis(triphenylphosphine) dichloride Pd complexes, formation of a hydride complex was suggested.

Acknowledgment. The authors sincerely thank Mr. I. Volkov for help in XPS analysis. The authors acknowledge financial support provided by the Max Planck Society and the Volkswagen Foundation. D.C. and L.B. also wish to thank the Russian Science Foundation (Grant No. 98-03-33372) for the support of this research.

CM991103N